GENERATION AND DYNAMICS OF MAGNETIZED ELECTRON BEAMS FOR HIGH-ENERGY ELECTRON COOLING *

P. Piot [1,2], Y.-E Sun[3]
[1] Department of Physics, Northern Illinois University DeKalb, IL 60115, USA
[2] Accelerator Physics Center, Fermi National Accelerator Laboratory, Batavia, IL 60510, USA
[3] Advanced Photon Source, Argonne National Laboratory, Argonne, IL 60439, USA

Abstract

Electron cooling of ion beams often requires the use of magnetized electron beams. In this paper we present an overview of the production and transport of magnetized and canonical-angular-momentum-dominated beams focusing both on experimental and theoretical aspects. We especially review past and planned experiments and discuss new ideas toward the formation and transport of high-current magnetized electron beams.

INTRODUCTION

The electron-cooling technique was developed by Budker [1] and subsequently tested at the Institute for Nuclear Physics (INP) in Novosibirsk, Russia [2, 3]. In this cooling scheme, a friction force results from the relative motion of ions immersed in an electron beam, which is co-moving with the same average velocity as the ions. The energy of the chaotic motion of the ions is transferred to the cold electron gas. The cooling rate can be improved by co-propagating the electron and ion beam inside a solenoid field and provided the electron beam is "magnetized". In a magnetized state, the electrons trajectories follow small helices around the magnetic field lines thereby increasing the interaction time and improving the cooling efficiency. The helices' Larmor radius is $\rho = m_e v_\perp/(eB)$ where $v_\perp$ is the electron velocity perpendicular to the magnetic field B, and m_e and e are respectively the electronic mass and charge. The magnetized state is characterized by a high ratio $\sigma_\perp/\rho \gg 1$ where $\sigma_\perp$ is the electron-beam rms transverse size.

The low-energy electron coolers explored to date have mostly used an electron accelerator fully imbedded in an axial magnetic field; see [4]. More recently, the electron cooling of a H^- beam in the RECYCLER storage ring at the Fermilab's TEVATRON complex was experimentally demonstrated and requires a relativistic cooling electron beam [5]. This led to the development of lumped optics: first a magnetized beam is produced from a thermionic cathode immersed in an axial magnetic field; then it is transported in an asymmetric optical lattice; (3) finally it is matched to a magnetized state into the long solenoid magnet composing the cooling section. Between the electron-source and cooling-section solenoids, the beam is not magnetized but has a large canonical angular momentum (CAM). A similar pproch is foreseen for future high-energy electron cooler [6, 7, 8]. We henceforth refer to this type of beams as "CAM-dominated beams" and view the magnetized state as a sub-class of CAM-dominated beams. Considering an axial magnetic field $B_z(z)$, the canonical angular momentum of an electron, L, in circular cylindrical coordinates (r, ϕ, z) is [9] $L = \gamma m r^2\dot{\phi} + \frac{1}{2}eB_z(z)r^2$, where γ is the Lorentz factor (here we take the beam to be relativistic so that a $\beta \equiv \sqrt{1-\gamma^{-2}} \simeq 1$). and $\dot{\phi} \equiv d\phi/dt$. Averaging the latter equation over the beam distribution gives the average beam's CAM

$$\langle L\rangle = 2\gamma m_e\langle r^2\dot{\phi}\rangle + eB_z\sigma_\perp^2, \tag{1}$$

where $\langle ...\rangle$ stands for the statistical averaging over the beam-density distribution. It is customary to introduce the magnetization $\mathcal{L} \equiv \langle L\rangle/(2\gamma m_e c)$. The envelope equation, ignoring acceleration effects, is [9, 10]

$$\sigma_\perp'' + k_l^2\sigma_\perp - \frac{K}{4\sigma_\perp} - \frac{\varepsilon_u^2+\mathcal{L}^2}{\sigma_\perp^3} = 0, \tag{2}$$

where $K \equiv \frac{2I}{I_0\gamma^3}$ is the generalized perveance, I and $I_0 \sim 17$ kA are respectively the beam and Alfvén currents, the Larmor's wavenumber $k_l \equiv \frac{eB_z}{2\gamma m_e c}$ accounts for the external focusing provided by a solenoidal lens, and ε_u is the geometric emittance. For a beam born and propagating in long uniform solenoid the envelope has an oscillatory envelope with mean value $\langle\sigma_\perp\rangle = \sigma_0$ where σ_0 is the initial rms beam size.

TRANSPORT & MANIPULATION

Besides their intricate formation process, magnetized beams have a very unusual beam dynamics due to the strongly coupled dynamics between the two transverse degrees of freedom. It was recently pointed out that this type of coupled beams could be elegantly described using the concept of eigen-emittances [11, 12, 13]. Mathematically, the transverse eigen-emittances are the eigenvalues of the 4×4 transverse beam matrix. Using this formalism, one can show that the transverse eigen-emittances associated to a CAM-dominated beam are unequal and can be categorized into an angular $\gamma\varepsilon_+$ and a cyclotron $\gamma\varepsilon_-$ emittances

$$(\gamma\varepsilon_+, \gamma\varepsilon_-) = \left(2\gamma\mathcal{L}, \frac{\gamma\varepsilon_u^2}{2\mathcal{L}}\right), \tag{3}$$

* Work supported the U.S. DoE Contract No. DE-FG02-08ER41532 with NIU and No. DE-AC02-07CH11359 with Fermilab.

where γ is the Lorentz factor an $\gamma\varepsilon_{\pm}$refer to normalized emittances. In the "laboratory" frame, the conventional transverse emittances are identical and given by $\gamma\varepsilon_x = \gamma\varepsilon_y = [(\gamma\varepsilon_u)^2 + (\gamma\mathcal{L})^2]^{1/2}$ as readily seen from Eq. 2.

Therefore the eigen-emittance concept provides a powerful tool to optimize the beam dynamics in a photoinjector. We have recently used this concept to optimize the generation of a CAM-dominated beam at the ASTA facility [14, 15, 16]. At ASTA, an RF gun electron source was designed to enable the production of CAM-dominated beams with large magnetization and low cyclotron emittance; see Fig. 1.

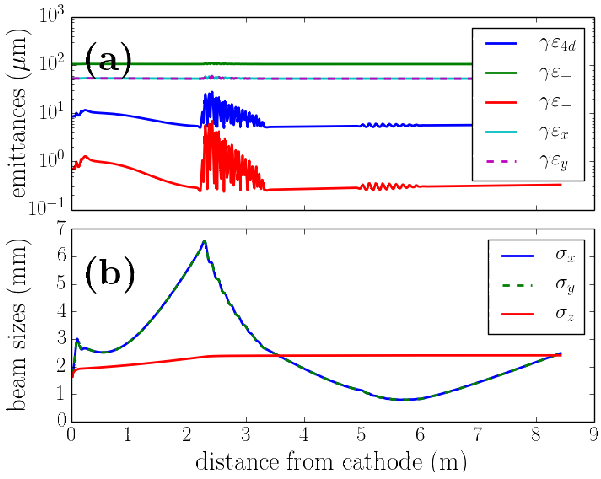

Figure 1: Example of evolution of transverse $\sigma_{x,y}$ and longitudinal σ_z rms beam sizes (a), angular $\gamma\varepsilon_+$ and cyclotron $\gamma\varepsilon_-$ emittances, horizontal $\gamma\varepsilon_x$ and vertical $\gamma\varepsilon_y$ "laboratory-frame" emittances (here $\gamma\varepsilon_y = \gamma\varepsilon_x$), and and four-dimensional emittance $\varepsilon_{4d} \equiv \gamma[\det(\Sigma)]^{1/4}$ (b) along the ASTA photoinjector. The bunch charge of $Q = 3.2$ nC and achieved parameters are consistent with requirements for high-energy electron coolers.

In an attempt to delineate CAM-dominated beam transformations, we introduce the transverse trace-space coordinates as $\widetilde{\mathbf{X}} \equiv (x, x')$ and $\widetilde{\mathbf{Y}} \equiv (y, y')$ where x and x' are the position and divergence coordinates and $\widetilde{\ }$ is the transpose operator. Following [17] we introduce the 2×2 correlation matrix such that $\mathbf{Y} = C\mathbf{X}$ and extend its definition to the statistical formalism as $C \equiv \langle \mathbf{Y}\widetilde{\mathbf{X}}\rangle\langle \mathbf{X}\widetilde{\mathbf{X}}\rangle^{-1}$ where $\langle \mathbf{X}\widetilde{\mathbf{X}}\rangle$ and $\langle \mathbf{Y}\widetilde{\mathbf{X}}\rangle$ are 2×2 blocks of the 4×4 beam matrix Σ. The form of the correlation matrix is constrained so that its elements are $C_{2,1} = -(1 + a^2)/b$ where $a \equiv C_{1,1} = -C_{2,2}$ and $b \equiv C_{1,2}$ which insures $|C| = 1$ [17]. The correlation matrix has very useful properties: for instance it transforms through system with transfer matrix $M = \begin{pmatrix} H & G \\ U & V \end{pmatrix}$ as

$$C_0 \to C = (U + VC_0)(H + GC_0)^{-1}. \qquad (4)$$

where C_0 is the initial correlation matrix and H, G, U, and V are 2×2 matrices. For a skewed beam line with unskewed transfer matrix $\begin{pmatrix} A & 0 \\ 0 & B \end{pmatrix}$, upon rotation by $\pi/4$ we have, for the skewed transfer matrix, $H = V = \frac{A+B}{2} \equiv M_+$ and $G = U = \frac{A-B}{2} \equiv M_-$, and the correlation matrix transforms as

$$C_0 \to C = (M_- + M_+C_0)(M_+ + M_-C_0)^{-1}. \qquad (5)$$

The latter equation indicates that the beam can be decorrelated ($C = 0$) when $M_- + M_+C_0 = 0$ is fulfilled; see [18, 19, 20]. This removal of angular momentum is realized by the mean of a skew-quadrupole section [21, 22]. In the process of this "round-to-flat-beam (RTFB)" transformation the eigen-emittances are mapped into conventional emittances so that the final (flat) beam emittance partition is $(\varepsilon_x, \varepsilon_y) = (\varepsilon_-, \varepsilon_+)$. This RFBT manipulation was experimentally pioneered at Fermilab where a transverse emittance ratio $\varrho \equiv \varepsilon_x/\varepsilon_y \sim 100$ was obtained [23].

CAM-DOMINATED-BEAM FORMATION

Typically, the formation of the required CAM-dominated beam is accomplished by immersing the cathode in an axial magnetic field; see Fig. 2. An emitted electron is thereby emitted in presence of an azimuthal vector potential $A_{\theta,0} = r/2B_{z,0}$ [where the subscript 0 indicates that the quantities are evaluated at the photocathode surface (taken to be at $z = 0$)] and has a canonical angular momentum $P_\theta = rA_\theta$. As the beam is transported into a magnetic-field-free region, the CAM is converted into kinetic angular momentum p_θ in virtue of the CAM conservation (since $P_\theta \equiv rA_\theta + p_\theta$ is conserved for cylindrical-symmetric systems). The acquired angular

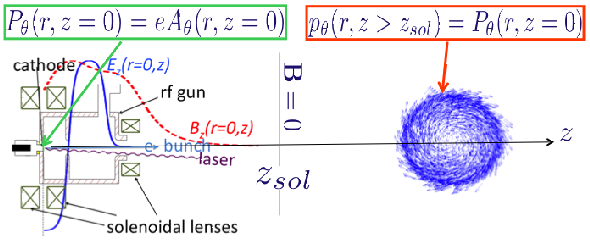

Figure 2: Overview of the CAM-dominated beam formation process in a photoinjector; see text for details. The red (B_z and blue E_z traces on the left schematics respectively represent the magnetic field applied by the slenoidal lenses and the axial field produced by the rf gun.

momentum $\mathbf{L} \equiv \mathbf{r} \times \mathbf{P}$ is $L = rP_\theta$ (where $L = \mathbf{L}.\hat{\mathbf{z}}$) Given the rms size of the cylindrical-symmetric emission area σ_c, we have $\langle L \rangle = eB_{z,0}\sigma_c^2$. The production of CAM-dominated beams is based on this process and was implemented in conventional electron coolers utilizing, e.g., DC thermionic sources; see Ref. [5]. The technique was also applied to the case of a photoemission electron source employing an RF gun [the experimental setup appears in Fig. 2 (left) and the experimental results can be found in [24]]. One advantage pertaining to the use of a

photoemission source stems from the ability to tune the emission source size (to control $\mathcal{L}$) and tailor the beam's transverse distribution using laser-shaping techniques to possibly optimize the cooling process as suggested in [25].

One of the most challenging aspects pertains to the production of high-current CAM-dominated beams suitable for further acceleration in a superconducting RF (SCRF) linac. A possible approach consists of using a DC electron source followed by a pre-acceleration section with appropriate chopper and buncher cavities. This technique is conventionally employed in high-current electron injectors [26]. Though robust, this scheme does not provide much flexibility and adds intricate longitudinal-phase-space (LPS) manipulations at low energies that might impact the preservation of the CAM.

A conventional normal-conducting (NC) RF gun operating at GHz frequencies would only allow for pulsed operations. The operation of conventional ($n + 1/2$ cells) guns with high-duty cycle is commonly achieved by going to low frequency [27]. However, none of these conventional NCRF guns have been operated in CW mode to date. CW operation (with, e.g., $\sim$ 30-MHz repetition rates needed the MEIC s high-energy electron cooling) would either require the use of a SCRF gun [28, 29, 30], or a low-frequency quarter-wave normal-conducting very-high-frequency (VHF) gun [31]. For both types of RF guns, the inclusion of a solenoid lens needed to the production of a magnetized beam appears challenging. In the case of the superconducting gun, a (possibly superconducting) solenoid magnet would have to include a flux concentrator to insure only the cathode experiences an axial magnetic fields and the background fields seen by the superconducting-cavity walls are below the critical field. Lower magnetic fields on the cathode can in principle be compensated by an increase in the emission-source size but at the expense of larger cyclotron emittances.

An alternative approach that could circumvent the use of an axial magnetic on the cathode relies on the use of a flat-to-round-beam (FRBT) transformation – the reverse of the RFTB transformation described above. Here we note that this transformation can in principle be reversed and an uncoupled beam with initial asymmetric transverse-emittance partition $(\gamma\varepsilon_x, \gamma\varepsilon_y)$ can be transformed into a CAM-dominated beam. In this process the final magnetization and cyclotron emittance are respectively given by $\gamma\mathcal{L} = \gamma\frac{\varepsilon_x - \varepsilon_y}{2}$, and $\gamma\varepsilon_- = \gamma\sqrt{\mathcal{L}^2 + \varepsilon_x\varepsilon_y} - \gamma\mathcal{L}$ assuming $\varepsilon_x \gg \varepsilon_y$. Therefore, a configuration utilizing a SCRF or VHF gun where an asymmetric cathode, e.g. a photocathode illuminated by a ribbon laser spot, could produce a beam with high transverse emittance ratios. The asymmetric-emittance beam would then be transformed downstream of the gun using a skew-quadrupole channel. This technique would circumvent the use of a solenoid field within the gun and could prove simpler than incorporating a small solenoid to magnetize the bunch as it is emitted in either the SCRF or VHF-gun designs. It is worth mentioning that the design of such an asymmetric-emittance electron source was considered in the context of e^+/e^- linear-collider designs and an emittance partition $(\gamma\varepsilon_x, \gamma\varepsilon_y) \simeq (29, 0.5)$ μm was simulated for a 4.8-nC bunch [32].

Lastly, we note that the formation CAM-dominated electron beam via photoemission excited by a laser with significant orbital-angular momentum (OAM) is also possible and could in principle mitigate the need for of a magnetic field on the cathode. Laser pulses carrying a large OAM (or "twisted laser") are an active field of research [33, 34]. The angular momentum is $L = im\hbar$ [35] (where m is an integer) and values up to $m \sim 1,000$ have been realized [36]. Such a value remains quite small compared to the angular momentum typically attained using the magnetized-beam technique: for the experimental results reported in [24], we have $\langle L \rangle \in [10, 100]$ eV.s which correspond to $\langle L \rangle \sim 10^7\hbar$. Therefore producing laser beams with adequately high OAM remains to be addressed.

TRANSVERSE DYNAMICS & MATCHING

Several cooling configurations employing magnetized beam have been proposed. Here we first discuss the case were a magnetized round beam is used in the cooling section. In such a case, given the cooling-section field B_{zs} (assumed to be uniform) and the value of the field on the cathode the conservation of the magnetic flux $\Phi_M \equiv \oint BdS$ implies the beam size in the cooling section σ_s^2 is the related to the size of the emission source via $B_{z,0}\sigma_c^2 = B_{z,s}\sigma_s^2$. Therefore the cathode-to-cooling section transverse transformation in the four-dimensional trace space $(\widetilde{\mathbf{X}}, \widetilde{\mathbf{Y}})$ can be described by a transfer matrix of the form

$$T = \begin{pmatrix} R & 0 \\ 0 & R \end{pmatrix}, \text{ with } R = \begin{pmatrix} \zeta & 0 \\ 0 & \zeta^{-1} \end{pmatrix}, \qquad (6)$$

where $\zeta \equiv \sqrt{B_{z,0}/B_{z,s}}$ is the magnification. Although the global transfer matrix is cylindrical symmetric, the lattice can be made of asymmetrically-focusing magnets [19].

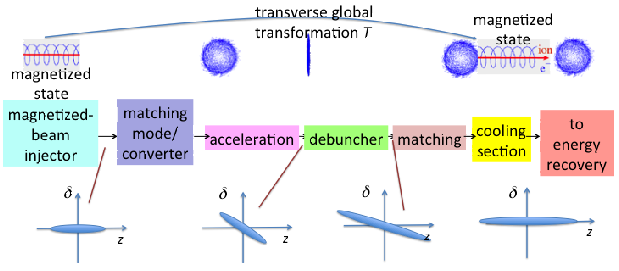

Figure 3: Block diagram (middle boxes) of possible transverse (upper plots) and longitudinal (lower plots) phase space manipulations required in a high-energy electron cooler.

A recent development in the context of the MEIC project concerns the use of a magnetized flat electron beams in the cooling section matched to the asymmetric shape of the

ion beams [7]. Such flat magnetized beam could be produced in a similar fashion as the one described above for round beams. One added complexity is that the angular momentum is not conserved for non axisymmetric beams and proper transverse transformations would have to be applied to recover the desired CAM prior to injection in the cooling section.

Depending on the symmetry of the applied external fields (sometime time-dependent), the CAM-dominated beam might need to be first transformed into a flat beam using a "mode converter" (RFBT) discussed earlier; see Fig. 3 (top diagrams). This type of transformation to uncoupled beams are needed prior to the longitudinal-phase-space (LPS) manipulations to avoid the introduction of time-dependent variation in the slice correlation matrix within a bunch.

Finally, the beam dynamics during the beam production and low-energy transport require detailed exploration to mitigate emittance dilution as attempted in Fig. 1 and in earlier work [37]. A generalized theory of emittance compensation for magnetized beam in RF photo injector was recently been formulated [38] and could provide guidance.

LONGITUDINAL DYNAMICS

High-energy coolers supporting the production of high-average-current beams necessitate the use of superconducting radio frequency (SCRF) linacs. Typical LPS requirements include bunch length matching the ion-beam length of a few cm and fractional momentum spread of 1-5 % [7, 8]. These longitudinal requirements together with the need for energy recovery require the use of intricate LPS manipulations illustrated in Fig. 3 (bottom diagrams).

The LPS (z, δ) gymnastics starts with the production of a bunched beam in the RF gun. The bunch length before the beam enters in the SCRF linac should be $\sigma_{z,inj} \ll \lambda_{rf}/(2\pi)$ where λ_{rf} is the linac operating wavelength. The beam acceleration occurs off crest so to impart a chirp $\mathcal{C}$ along the bunch. A dispersive section (debuncher) with longitudinal dispersion R_{56} elongates the bunch so that its final length $\sigma_{z,f} = \sigma_{z,inj}(1 + R_{56}\mathcal{C})$ matches the ion-bunch length $\sigma_{z,ion}$. Finally, an accelerating-mode cavity operated at zero crossing removes the final correlated energy spread. Assuming conservation of the longitudinal emittance, the final uncorrelated fractional energy spread is $\sigma_{\delta,f} \simeq \sigma_{z,inj}\sigma_{\delta,inj}/\sigma_{z,f}$. For an L-band photoinjector one typically has $\sigma_{\Delta E,inj} \simeq 3$ keV for a 1-nC bunch with $\sigma_{z,inj} \simeq 1$ mm [39] resulting in a final fractional momentum spread of $\sigma_{\delta,f} \leq 10^{-5}$ at 50 MeV. In practice nonlinearities associated to the manipulations of the long electron bunch might limit the minimum achievable energy spread and would have to be corrected.
The described LPS staged manipulation does not present significant challenges in itself: very similar schemes have been implemented in, e.g., energy-recovery linacs used to drive high-power free-electron lasers [40, 41]. But the combination of these LPS manipulations with highly-coupled beams and their ability to preserve correlations in a CAM-dominated beams remained to be experimentally and numerically investigated.

EXPERIMENTAL OPPORTUNITIES AT THE FERMILAB'S ASTA FACILITY

Further experiment on CAM-dominated beam generation are planned in the photoinjector of the Fermilab's Advanced Superconducting Test Accelerator (ASTA) [14]. The photoinjector was designed to enable the production of beams with large CAM by incorporating a large bucking solenoid. The injector has all the ingredient to form and characterize CAM-dominated beam and explore their conversion to flat beam and their longitudinal manipulation using a dispersive section that can act as a decompressor; see Fig. 4. Although the SCRF linac (CAV1 and CAV2 in Fig. 4) operate at a higher frequency (1.3 GHz) than the contemplated frequency of the high-energy electron cooler SCRF linac (most probably around 200 MHz), we expect the single-bunch beam parameters to be consistent with the ones required for high-energy electron cooling. The semiconductor cathode used at ASTA (Cs_2Te) has demonstrated charges in excess of 10 nC. We anticipate a first set of experiment to focus on the transport of high-charge CAM-dominated beams and their possible transformation into a flat beam as would be needed, e.g., prior to the high-energy cooler debuncher. Previous CAM-dominated beam formation performed at Fermilab's A0 facility were limited to low charge (the RFBT was studied at 0.5 nC only) due to the limited energy ($\sim$ 15 MeV).

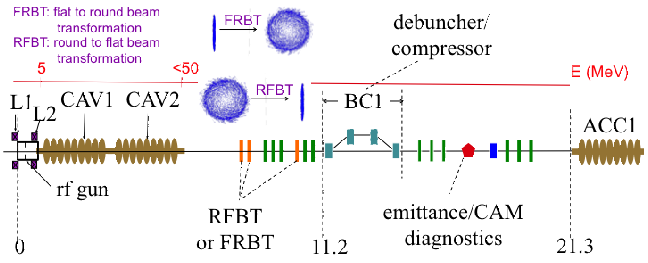

Figure 4: Overview of the ASTA photoinjector. The legend is as follows "L1" and "L2" are solenoids, "CAV1", "CAV2" and "CAV39" are SRF accelerating cavities, "RFTB" (reps. "FRBT") is the round-to-flat (resp. flat-to-round) beam transformer, "BC1" is a magnetic bunch-compressor chicane.

A foreseen experiment includes the measurement of the eigen-emittances that can in principle be done by furthering the technique developed in Ref. [24] to measure the kinetic angular momentum. Such a measurements performed for different bunch charges together with the measurement of the magnetization would provide insights on

ways to optimize the injector settings. For instance, exploring the evolution of the cyclotron. Furthermore, exploring the conversion of the CAM-dominated beams into flat beams using the RFBT available at ASTA as function of bunch charges, correlated energy spread (imparted by CAV2), and beam energy would provide relevant data that could guide some design consideration for the high-energy electron cooler. For instance the study might provide input to select the possible location of the RFBT necessary prior to the debunching process. Finally, attempting the transport of CAM-dominated or flat beam through the BC1 dispersive section to decompress the beam could shed some light on the decompression process and its limitations. A possible study involves the measurement of the the final beam parameters as a function of the decompression factor. In addition to measuring the beam emittance, several bunch length diagnostics are available at ASTA including a Martin-Pupplet interferometer [42] (for bunch length in the picosecond regime) and an optical streak camera [43] (capable of measuring much longer bunch lengths up to several centimeters).

CONCLUDING REMARKS

We have summarized some of the challenges associated to the formation and transport of CAM dominated electron beams needed for high-energy electron coolers. Single bunch parameters consistent with, e.g., MEIC requirements (for a charge $Q \simeq 2$ nC) appear within reach using a photoinjector configuration [24]. The major challenge pertains to the needed high-current. Although the demand on average current has been substantially decreased to $\langle I \rangle \leq 50$ mA (by incorporating a "circulator cooler ring" [6] to stack electron bunches and match the ion-beam repetition rate [7]), significant technical developments are needed. In addition understanding the interplay between the required LPS manipulations and the preservation of transverse correlations is critical to producing high-magnetization, low-cyclotron-emittance beams in the cooling section. Experimental tests to address some of these beam-dynamics issues are planned at Fermilab's ASTA facility.

We would like to thank the EIC'14 scientific committee for giving us an opportunity to present this work. We are grateful to Dr. Lidia for sharing his unpublished work [10].

REFERENCES

[1] G. I. Budker, Soviet Atomic Energy, **22** (5), 438 (1967).

[2] V.N. Bocharov, et al. Nucl. Instr. Meth. A **441**, 87 (2000).

[3] Ya. Derbenev, Proc. of EIC14 and references therein (2014).

[4] V. Parkhomchuk, A. Skrinskii, Phys. Uspekhi **43** (5) (2000).

[5] S. Nagaitsev, et al. Phys. Rev. Lett. **96** 044801 (2006).

[6] S. Abeyratne, et al. [MEIC collaboration], arXiv:1209.0757 [physics.acc-ph] (2012).

[7] Ya. Derbenev, et al., Proc. of COOL'13, Murren, Switzerland, 68, (2013).

[8] I. Ben-Zvi, et al., Proc. of PAC'01, 48 (2001). s

[9] M. Reiser, *Theory and Design of Charged Particle Beams* (John Wiley & Sons, inc., 1994).

[10] S. M. Lidia, "Emittance compensation of intense, magnetized beams and optimization of photo injector", LUX Tech Note-012 (2004); (unpublished) available from S. Lidia at Michigan State University.

[11] F. Neri, et al., Phys. Rev. A **45**, 2572 (1992).

[12] K. Kubo, "how to calculate 'intrinsic' emittances from 4D beam matrix", ATF-99-02 (1999); available from KEK.

[13] A. Dragt, *Lie Methods for Nonlinear Dynamics with Applications to Accelerator Physics*, College Park: unpublished (2013).

[14] P. Piot, et al., arXiv:1304.0311 [physics.acc-ph] (2013).

[15] P. Piot, et al., Proc. of IPAC13, 2003 (2013).

[16] J. Zhu, et al., preprint FERMILAB-PUB PUB-14-103-AD-APC (2014).

[17] E. Thrane, et al., Proc. LINAC02, 308 (2002).

[18] Ya. Derbenev, University of Michigan Report No. UM-HE-98-04 (1998).

[19] A. Burov, S. Nagaitsev and Ya. Derbenev, Phys. Rev. E **66**, 016503 (2002).

[20] K.-J. Kim, Phys. Rev. ST Accel. Beams **6**, 104002 (2003).

[21] A. Burov and V. Danilov, FNAL Report No. TM-2043, (1998).

[22] R. Brinkmann, Y. Derbenev and K. Flöttmann, DESY Report No. TESLA 99-09 (1999).

[23] P. Piot, et al. Phys. Rev.ST Accel. Beams **9**, 031001 (2006).

[24] Y.-E. Sun, et al. Phys. Rev. ST Accel. Beams **7**, 123501 (2004).

[25] A. Ivanov, et al., Proc. of EPAC02, 1356 (2002).

[26] R. Abbott, et al., Proc. of LINAC'94, 777 (1994).

[27] D. H. Dowell, et al., Appl. Phys. Lett. **63**, 2035 (1993).

[28] A. Arnold, et al., Nucl. Instr. Meth. in Phys. A **577**, 440 (2007).

[29] J. Bisognano, et al., Proc. of PAC2013, 622 (2013).

[30] J. R. Harris, et al. Phys. Rev. ST Accel. Beams, **14** 053501 (2011).

[31] F. Sannibale, et al., Phys. Rev. ST Accel. Beams, **15**, 103505 (2012).

[32] J. B. Rosenzweig, Proc. of PAC'91, 1987 (1991).

[33] G. Molina-Terriza, et al., Nat. Phys. **3**, 305 (2007).

[34] M. Padgett and R. Bowman, Nat. Photonics 5, 343 (2011).

[35] L. Allen, et al. Phys. Rev. A **45**, 8185 (1992).

[36] J. E. Curtis, et al., Opt. Commun. **207**, 169 (2002).

[37] X. Chang, et al., in AIP Conf. Proc. **737** (AAC'04), 462 (2004).

[38] C.-X. Wang, et al., Proc. of FEL06, 721 (2006).

[39] M. Hüning, et al., Proc. PAC03, 2074 (2003).

[40] G. R. Neil, et al., Phys. Rev. Lett. **84**, 662 (2000).

[41] P. Piot, et al. Phys. Rev.ST Accel. Beams **6**, 030702 (2003).

[42] R. Thurman-Keup, et al. , Proc. of BIW08, 153 (2008).

[43] A. Lumpkin, et al., Nucl. Instr. Meth. A **687**, 92 (2012).